Electrochimica Acta 87 (2013) 599–605

Contents lists available at SciVerse ScienceDirect

Electrochimica Acta

journal homepage: www.elsevier.com/locate/electacta

Pyrolyzed iron-triethylenetetramine on carbon as catalyst for oxygen reduction reaction

Hui-Juan Zhang[a], Xianxia Yuan[b,*], Zhenhao Wang[a], Junhe Yang[a], Zi-Feng Ma[b,*]

[a] School of Materials Science and Engineering, University of Shanghai for Science and Technology, Shanghai 200093, China
[b] Department of Chemical Engineering, Shanghai Jiao Tong University, Shanghai 200240, China

ARTICLE INFO

Article history:
Received 10 June 2012
Received in revised form 8 October 2012
Accepted 8 October 2012
Available online xxx

Keywords:
Oxygen reduction reaction
Non-noble metal catalysts
Heat-treatment temperature
Methanol-tolerance
Stability

ABSTRACT

In this study, a series of Fe-based non-noble metal and non-macrocycle catalysts, FeTETA/C, for oxygen reduction reaction (ORR) have been synthesized by pyrolyzing carbon-supported iron triethylenetetramine chelate at various temperatures in an inert atmosphere. Electrochemical characterization revealed that heat treatment temperature plays an essential role on improving the catalytic property of the obtained catalysts for ORR, and the optimal could be achieved at 800 °C with an ORR peak potential of 0.751 V and an electron-transfer number of 3.85. Furthermore, the obtained optimal catalyst has excellent methanol-tolerance and acceptable acid-resistance. The effects of heat treatment temperature on microstructure of the catalysts as well as the elemental state on the optimal catalyst surface have been investigated using X-ray diffraction (XRD), transmission electron microscopy (TEM) and X-ray photoelectron spectroscopy (XPS).

1. Introduction

There are two types of electrodes in H_2–O_2 proton exchange membrane fuel cells (PEMFCs): one is the anode for hydrogen oxidation reaction and the other is the cathode for oxygen reduction reaction (ORR). To achieve practical applications, efficient catalysts must be used to promote the slow reactions at these electrodes. So far, the most effective catalysts for these electrodes have been proved to be Pt and its alloys. Considering the need of higher Pt loading at the cathode than at the anode because of the sluggish ORR, along with the high cost and limited resources of Pt, it will be more advisable to replace Pt-based catalysts by non-precious metal catalysts at the cathode of PEMFCs [1].

Numerous efforts have been made to develop non-noble metal catalysts in order to replace the Pt-based catalysts. Since the discovery of the beneficial effects of heat treatment in inert atmosphere on improving the catalytic activity and chemical stability in 1976 by Jahnke et al. [2], transitional metal macrocycle complexes (metal-N_4 chelates), such as metalloporphyrins and metallophthalocyanines, adsorbed on carbon support and heat-treated in an inert atmosphere, have been widely studied as promising alternative catalysts [3–6]. At the same time, the non-noble metal catalysts obtained from heat treatment of iron tripyridyltriazine complexes and cobalt di-quinolyldiamine derivatives, respectively [7,8] or the heat-treated mixture of transitional metal salts and nitrogen-containing precursors, such as polyacrylonitrile and polypyrrole [9–12], NH_3 and CH_3CN [13,14] have also been paid much attentions in recent years. On the whole, the catalytic activity of these nitrogen-containing non-noble metal catalysts mainly depends on: (1) the nature of the metal and its precursor as well as the nature of the nitrogen precursor, and (2) the pyrolysis temperature. As far as the second point, pyrolysis temperature, is concerned, worldwide researchers have gained different results when using different metals and nitrogen precursors. For example, the catalytic activity of the catalysts prepared from cobalt acetate and tetramethoxyphenylporphyrin (TMPP), reached a maximum at 900 °C [4], while the maximum activity was obtained after heat treatment at 700 °C when the nitrogen precursor was pyrrole [10].

Recently, we have developed a Co-based non-precious metal catalyst for the ORR employing triethylenetetramine (TETA), a simple and cheap ligand, as nitrogen resource [15,16]. Furthermore, we comparatively studied the effects of various 3d transitional metals on ORR catalytic performance of this type of catalysts, and found that the 3d transitional metal played an important role on the catalytic activity [17]. We also investigated the binary FeCo-based catalyst which displayed an improved catalyst activity [18]. In this paper, we especially focus on the influence of heat treatment temperature on the catalytic activity and structure of the FeTETA/C catalysts. The catalytic activities were demonstrated by cyclic voltammograms (CVs), rotating disk electrode (RDE) measurements as well as rotating ring-disk electrode (RRDE)

* Corresponding authors. Tel.: +86 21 54742827; fax: +86 21 54741297.
E-mail addresses: yuanxx@sjtu.edu.cn, yuanxx519@yahoo.com.cn (X. Yuan), zfma@sjtu.edu.cn (Z.-F. Ma).

0013-4686/$ – see front matter © 2012 Elsevier Ltd. All rights reserved.
http://dx.doi.org/10.1016/j.electacta.2012.10.019

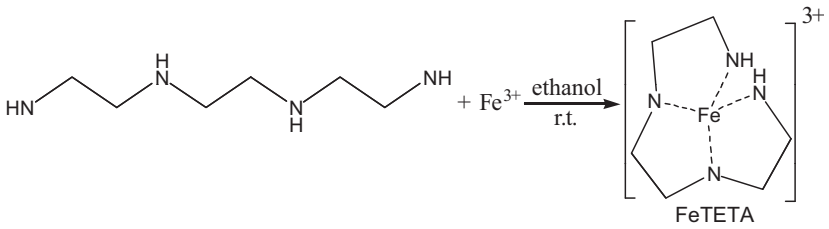

Fig. 1. Schematic illustration of the proposed reaction of the FeTETA, coordination of a single TETA chain as a ligand is also anticipated.

measurements in oxygen-saturated acidic solution. Thermogravimetry analysis (TGA) was applied to analyze the pyrolyzing process. The physical characteristics of the catalysts were examined by X-ray diffraction (XRD), transmission electron microscopy (TEM) and X-ray photoelectron spectroscopy (XPS).

2. Experimental

2.1. Catalyst preparation

A series of FeTETA/C catalysts were prepared similar to that described elsewhere [15,16]. Briefly, 0.4840 g iron chloride ($FeCl_3$) was dissolved in ethanol at room temperature. Next, 1.0 mL of triethylenetetramine (TETA) was added into the above solution to form the FeTETA chelate, as shown in Fig. 1. Then, 1.0 g of commercially obtained carbon black (Black Pearl 2000, Cabot Corporation, USA) was added to the mixture under vigorous stirring. The carbon-supported suspension was stirred for 1 h and then dried to remove ethanol by rotary evaporator. The resulted powders were divided into five equal parts and heat-treated in Ar atmosphere for 90 min at the temperature of 600 °C, 700 °C, 800 °C, 900 °C and 1000 °C, respectively. For convenience, the FeTETA/C catalysts heat-treated at various temperatures are hereafter labeled as HT600, HT700, HT800, HT900 and HT1000.

The HT800 catalyst was leached in 0.5 M H_2SO_4 for 10 days in an ultrasonic bath. Then, the resulting sample was filtered, washed, and dried for electrochemical measurements to evaluate the acid-resistance ability. The resulted leached HT800 catalyst is hereafter denoted as HT800-H_2SO_4.

2.2. Physical measurements

TGA experiment was performed on a Netzsch simultaneous thermal analyzer STA449F3 in Ar atmosphere with the heating rate of 5 °C min^{-1}. XRD was performed on an automated Rigaku diffractometer equipped with a Cu $K\alpha$ radiation at a tube current of 30 mA and a tube potential of 40 kV. Data acquisition was recorded in the scanning angle range of 20–80° at a scan rate of 6° min^{-1}. The PDF (powder diffraction file database) from the ICDD (International Center for Diffraction Data) was used as a reference to interpret peak assignments on the XRD spectra. TEM measurements were performed at a JEOL JEM-2010 operating at 200 keV. The catalyst was ultrasonically dispersed in absolute ethanol for 5 min. A drop of the solution was then deposited onto a carbon-coated copper grid and left in air to dry. Electronic states of various elements on the catalyst surface were evaluated with XPS, which was carried out on a RBD upgraded PHI ESCA 5700 system (Physical Electronics) with Al $K\alpha$ radiation ($h\nu$ = 1486.6 eV). The sample was directly pressed to a self-supported disk (10 mm × 10 mm) and mounted on a sample holder then transferred into the analyzer chamber. Binding energies were calibrated by using the containment carbon (C 1s = 284.5 eV). The data analysis was carried out by using XPS-Peak4.1 provided by Raymund W.M. Kwok (The Chinese University of Hongkong, China).

2.3. Electrochemical measurements

Electrochemical characterizations were carried out in a conventional three-electrode cell filled with 0.5 M H_2SO_4 solution. A glassy carbon disk (4.0 mm in diameter) was used as the working electrode. The counter electrode was a Pt wire, and the reference electrode was a saturated calomel electrode. All potentials reported in this paper are referred to the standard hydrogen electrode (SHE). The catalyst ink was prepared by ultrasonically dispersing 5 mg catalyst powder in 0.5 mL high-purity water and 50 μL 5 wt% Nafion solution for 5 min. Then 10 μL of this ink was deposited onto the disk electrode and air-dried for use.

CVs and RDE experiments were performed in oxygen-saturated 0.5 M H_2SO_4 solution at the potential scanning rate of 5 mV s^{-1} with a glassy carbon disk electrode. The CVs were recorded within the potential range from 1.04 V to 0.04 V, and the current–potential polarization curves of RDE study were obtained at an electrode rotating speed of 900 rpm. For RRDE experiments, a Pt ring-Pt disk electrode was employed, the catalyst ink was dropped onto the disk only, the ring potential was kept at 1.2 V and the disk potential was scanned at a rate of 5 mV s^{-1}. Methanol-tolerance experiments were carried out in oxygen-saturated 0.5 M H_2SO_4 + 1 M CH_3OH solution at the potential scanning rate of 5 mV s^{-1}.

All electrochemical measurements were operated using a 750A biopotentiostat (CHI instrument, USA) along with a 636 RRDE system (Pine instrument, USA) at room temperature. It should be noticed that all the CVs and polarization curves are given as current vs. E plots, instead of current density vs. E since the real surface of the ink-type electrode is uncertain.

3. Results and discussion

The TGA and c-DTA curves obtained from pyrolysis of the catalyst precursor in Ar atmosphere with a heating rate of 5 °C min^{-1} was presented in Fig. 2. Three steps could be observed. The first

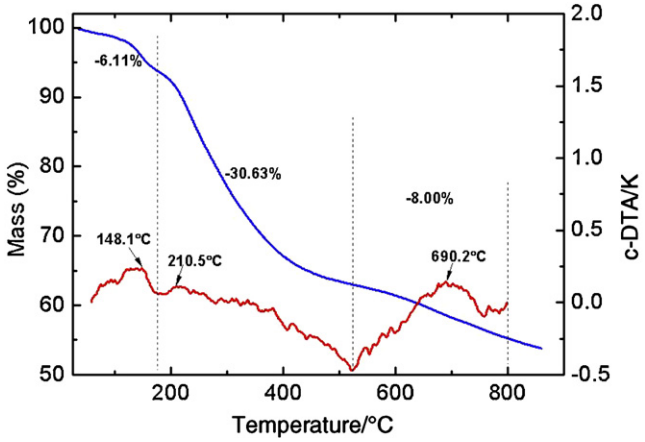

Fig. 2. TG and c-DTA analysis of the catalyst precursor in Ar atmosphere at a heating rate of 5 °C min^{-1}.

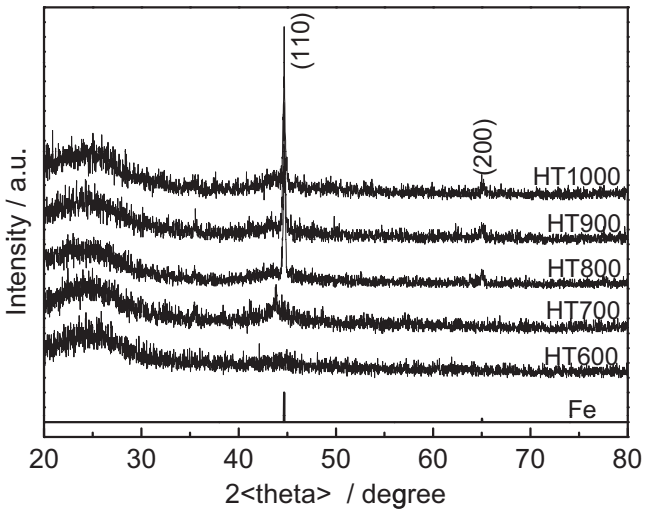

Fig. 3. XRD patterns of the FeTETA/C catalysts heat-treated at various temperatures along with the standard data of metallic Fe.

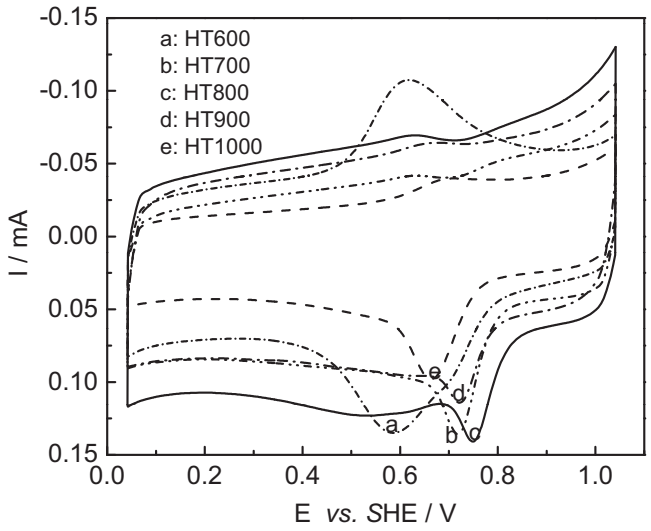

Fig. 5. Cyclic voltammograms of the FeTETA/C catalysts heat-treated at various temperatures in oxygen-saturated 0.5 M H_2SO_4 solution. Potential scan rate: 5 mV s^{-1}.

one starts at 25 °C and reaches a plateau at about 175 °C. It represents a weight loss of 6.11 wt% and a c-DTA at 148.1 °C, which can be assigned to the detachment of TETA from the surface of carbon. The second step appears from 175 °C to 524 °C with a weight loss of 30.63 wt%, it might be the release of FeTETA on the carbon surface. The third step is the decomposition of FeTETA chelate starting from 524 °C to form the catalytic active sites. Therefore, the heat treatment temperatures for synthesizing the FeTETA/C catalysts have been selected as 600 °C, 700 °C, 800 °C, 900 °C and 1000 °C.

XRD patterns of the obtained catalysts are presented in Fig. 3. The large broad peaks observed at 2θ of about 25° for all the catalysts could be attributed to the diffraction of C(0 0 2). HT600 shows no additional diffraction peaks. HT700 shows only a weak broad diffraction feature of Fe(1 1 0), while the other catalysts, including HT800, HT900 and HT1000, reveal the typical characteristic diffraction features of Fe(1 1 0) and Fe(2 2 0). This suggests that the iron in the catalysts of FeTETA/C pyrolyzed in the temperature range from 800 °C to 1000 °C is mainly metallic Fe with high crystallization, while the iron in HT700 has not been well crystallized and 600 °C is probably not high enough to convert trivalent iron into metal. A visual confirmation of the presence of metallic Fe is given in Fig. 4, a low-resolution TEM micrograph with the catalyst of HT800 as an example at different multiple: (a) 100 nm, (b) 50 nm and (c) 20 nm. In this figure, the gray area is attributed to the basic macrostructure of amorphous carbon framework and the dark spots correspond to the metallic Fe crystallites.

Fig. 5 shows the CV curves of the FeTETA/C catalysts in oxygen-saturated 0.5 M H_2SO_4 solution. It is a traditional way to represent the relative catalytic activity of catalysts with the ORR peak potential where the maximum oxygen reduction current occurs. As shown in Fig. 5, the ORR peak potential changes with the heat treatment temperature: 0.589 V for HT600, 0.719 V for HT700, 0.751 V for HT800, 0.725 V for HT900, and 0.664 V for HT1000. On the other hand, the ORR peak current also changes with the same trend, 0.135 mA for HT600, 0.136 mA for HT700, 0.141 mA for HT800, 0.114 mA for HT900, and 0.098 mA for HT1000. Therefore, it could be figured out that heat treatment temperature has significant influence on ORR catalytic activity of the FeTETA/C catalysts, the catalytic activity increases with increase in heat treatment temperature and reaches the maximum at 800 °C, then it decreases with further increase in the heat treatment temperature. Another significant feature is an obvious shift to higher values of the ORR potential (e.g. 0.751 V for HT800), as compared to the reported values for PAN-Fe (0.60 V) [9] and the CoTETA/C (0.71 V) [19]. In addition, an anodic peak could be found at about 0.615 V in the CV curve of HT600, implying some oxidative reactions other than oxygen reduction. It is probably because of the nonmetallic Fe resulted from heat treatment at 600 °C as discussed above.

Current–potential curves obtained from RDE experiments for the FeTETA/C catalysts are depicted in Fig. 6. The catalyst of HT800 demonstrates a higher ORR onset potential than the other studied catalysts. The activity of the catalysts grows with the increase

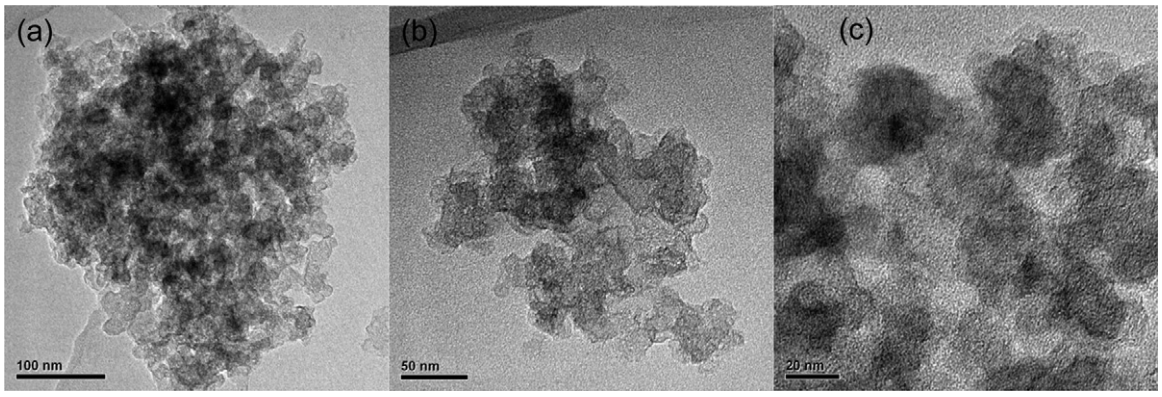

Fig. 4. TEM images of the catalyst HT800 with diverse multiples: 100 nm (a), 50 nm (b) and 20 nm (c).

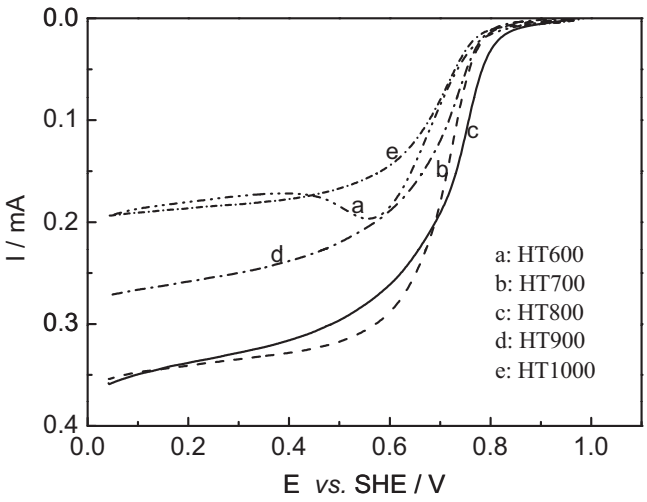

Fig. 6. Current–potential curves for the ORR on the FeTETA/C catalysts heat-treated at various temperatures in oxygen-saturated 0.5 M H_2SO_4 solution. Scan rate: 5 mV s^{-1}. Electrode rotation rate: 900 rpm.

of the heat treatment temperature, and then decays from 800 °C where the best performance is achieved. This agrees very well with the results of CV experiments. Compared with our previous studies on CoTETA/C catalyst [15,16], the mass transport contributions is less significant at lower potentials. However, a similar shape of the polarization curves has been reported elsewhere for carbon-supported metallic macrocycles and other non-precious metal catalysts [2,3,7,11,15,16,20,21]. The feature that all of the catalysts prepared here have no well-defined diffusion-limiting current plateau means non-uniform distribution of active sites and slow oxygen reduction rate on these catalysts [20,21]. In addition, only a current peak could be observed for the catalyst of HT600 at approximately 0.65 V. The probable reason could be elucidated with the following facts. As discussed above with the XRD results, 600 °C is probably not high enough to convert trivalent iron into metallic iron, leading to less catalytic active sites toward ORR in the catalyst and a less porous electrode limiting the oxygen transportation at the electrode/electrolyte boundary and the oxygen penetration in the electrode. For the other catalysts, however, trivalent iron in the precursor of $FeCl_3$ has been reduced into nanometallic iron, which plays important role for enhancing the catalytic activity, leading to more porous structure in the corresponding catalyst and electrode favorable to smooth and fast oxygen diffusion.

According to the above discussion on CVs and RDE results, it could be concluded that the FeTETA/C catalyst prepared at 800 °C has the best ORR catalytic performance. Therefore, the HT800 catalyst is chosen for further detailed study in the following sections on surface elemental state, ORR mechanism, and methanol and acid tolerance.

Fig. 7 shows the electronic states of various elements on the surface of the optimal catalyst HT800 obtained from XPS. In Fig. 7(a), it clearly shows a predominant C 1s peak at about 285 eV, a weak O 1s peak at 532 eV and a much weaker N 1s peak at 400 eV. It could be found in the high-resolution C 1s spectra (Fig. 7(b)) that the C 1s peak shifted to a higher binding energy of 284.8 eV as compared to the reported value of 284.5 eV for a number of carbon supports such as Norit SX Ultra [22] and Vulcan XC-72R [23]. This could be attributed to the adulteration of nitrogen atoms and oxygen species on the carbon support. In addition, close observation of Fig. 7(b) reveals three peak components at 284.8 eV, 285.4 eV and 288.3 eV, which could be assigned to the carbon component in C—C, C—O and O=C—O, respectively. Several types of N coordination with close binding energies have been reported in literatures [24]: (1) pyridinic N at 398.3–399.5 eV; (2) pyrrolic N at 399.9–400.7 eV; and (3) graphitic N at 401–403 eV. However, the XPS of N 1s in the HT800, displayed in Fig. 7(c), can only be deconvoluted into pyridinic N and pyrrolic N with the contributions of 68% and 32%, respectively. According to Sidik et al.'s study on cluster models of graphite sheets containing substitutional N toward oxygen reduction reaction in acidic media [25], pyridinic N has one lone pair of electrons in addition to the one electron donated to the conjugated π bond system, imparting a Lewis basicity to the carbon, and it is capable of facilitating the reductive adsorption reaction of O_2 without the irreversible formation of oxygen functionalities, due to an increased electron-donor property of carbon. Similar to the investigation on Co-based cathode catalyst by Subramanian et al.'s [26,27], the XPS O 1s narrow-scan spectra presented in Fig. 7(d) can be divided into two components: O_A at a binding energy of 531.8 eV assigned to C=O (aldehydes, ketones and lactones) and O_B at 533.3 eV assigned to the C—OH and/or C—O—C groups. Moreover, the fact that O_A content is obviously larger than that of O_B implies more C=O functional group than C—OH and/or C—O—C groups on the HT800 surface.

Fig. 8 gives (a) the RRDE experimental data of the HT800 in oxygen-saturated H_2SO_4 solution at an electrode rotating speed of 900 rpm and (b) the calculated number of electrons transferred per oxygen molecule (n) and the corresponding hydrogen peroxide yield (%H_2O_2) with the following equations [20,21]:

$$n = \frac{4I_d}{I_d + I_r/N} \quad (1)$$

$$\%H_2O_2 = \frac{100 \times (4 - n)}{2} \quad (2)$$

$$\%H_2O_2 = \frac{100 \times (2I_r/N)}{I_d + I_r/N} \quad (3)$$

Here, I_r is the current on the ring electrode, I_d is the current on the disk electrode, and N is the collection efficiency of the RRDE. Considering that the values of I_d and I_r are too small when potential is larger than 0.6 V leading to huge error [28], the valid potential range is usually chosen from 0.1 V to 0.6 V. In this potential range, it can be found that the number of transferred-electron is about 3.85, and the H_2O_2 yield is about 8%. This implies that the catalyzed ORR by HT800 proceeds by both two-electron-transfer reduction and four-electron-transfer reduction but the latter predominates.

Methanol crossover is a main issue of direct methanol fuel cell (DMFC), which is a member of PEMFCs. During the working of DMFC, there is not only the occurrence of ORR at the cathode, but also simultaneous oxidation of the methanol transferred from the anode through the membrane. The latter is found to seriously reduce the operating voltage and power output of DMFC. Therefore, an efficient cathode catalyst should be methanol tolerant in addition to high ORR catalytic activity. Fig. 9 shows the CVs (a) and the RDE polarization curves (b) of oxygen reduction on the HT800 catalyst in both oxygen-saturated 0.5 M H_2SO_4 solution and 0.5 M H_2SO_4 + 1.0 M CH_3OH solution, respectively. No apparent difference could be found in the ORR peak potential and peak current in CV curves, indicating that the presence of methanol does not obviously affect the catalytic activity of HT800. Similarly, the RDE data in the oxygen-saturated 0.5 M H_2SO_4 solution and 0.5 M H_2SO_4 + 1.0 M CH_3OH solution are almost the same. So, it could be figured out that the HT800 catalyst has excellent methanol-tolerance ability in addition to its high ORR activity, and it can be used as the efficient cathode catalyst in DMFC.

Stability is a very important characteristic for fuel cell catalysts. Considering the acidic environment in PEMFCs, the catalytic activity of HT800 before and after leaching in 0.5 M H_2SO_4 for 10 days has been comparatively studied in this work, the results are shown in Fig. 10. There is no notable change in the ORR peak potential

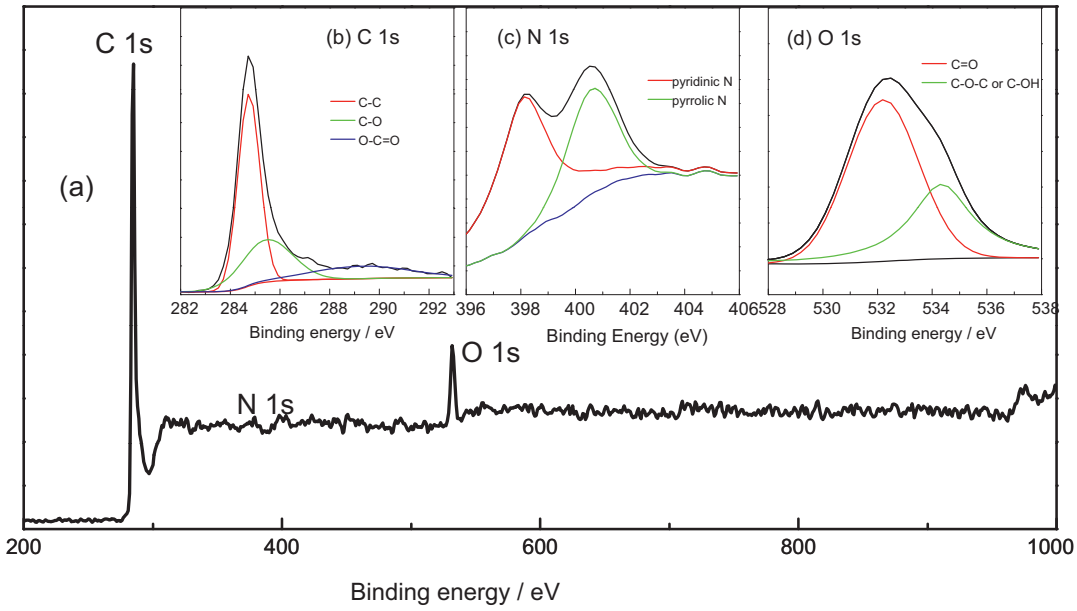

Fig. 7. XPS of the catalyst HT800: (a) the survey spectrum, (b) C 1s, (c) N 1s and (d) O 1s.

and peak current for the catalysts of HT800-H_2SO_4 and HT800: 713 mV and 0.116 mA for HT800-H_2SO_4, and 717 mV and 0.122 mA for HT800. However, the current of the HT800-H_2SO_4 catalyst is slightly lower than that of the HT800 catalyst in the potential region lower than 600 mV. Therefore, it could be considered that the optimal HT800 catalyst exhibits acceptable acid-resistance and stability.

In order to accelerate the future development of the FeTETA/C catalyst, it is essential to well understand and elucidate the mechanism of the catalyzed oxygen reduction reaction. In the published literatures, the nature of the active sites in the Fe-based nitrogen-containing non-noble metal catalysts (Fe-N/C) toward ORR remains intricate, many controversial opinions have been presented. For example, Chung et al.'s research [29] on cyanamide-derived Fe-N/C catalysts revealed that although nitrogen content has been previously correlated positively with ORR activity [30], no such trend was observed in their work for any type of nitrogen type, while the combined effects of nitrogen and sulfur incorporation into the carbon may account for the high activity. Lefèvre et al.'s study on Fe-N/C catalysts showed that two different catalytic sites, namely FeN_4/C and FeN_2/C, exist simultaneously in all the catalysts made with the Fe salt or the Fe porphyrin, and the FeN_2/C

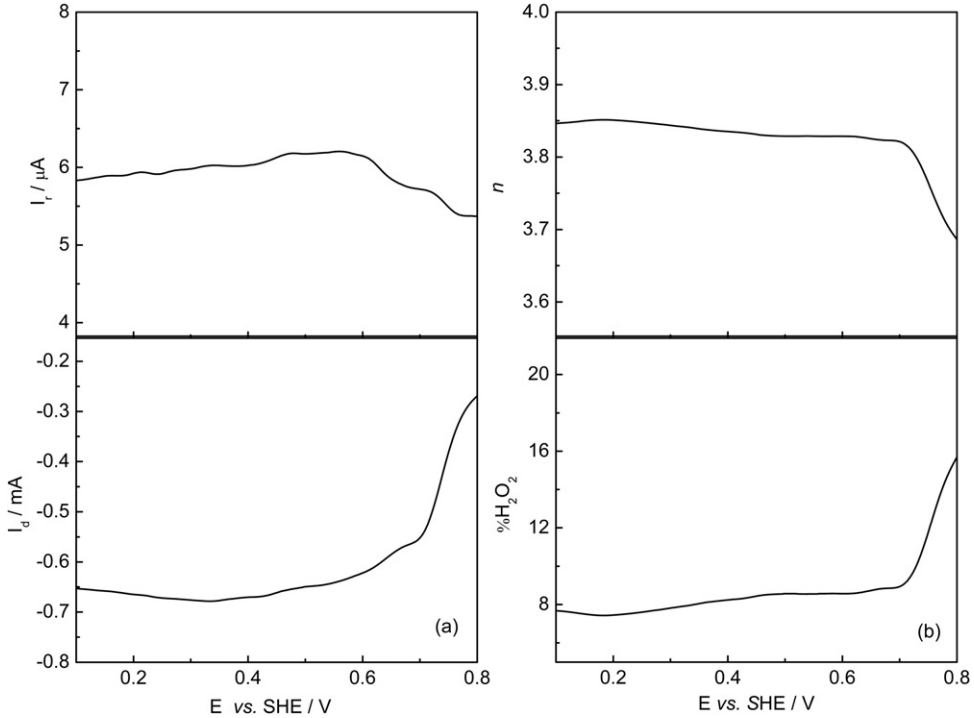

Fig. 8. (a) RRDE data of the catalyst HT800 in oxygen-saturated 0.5 M H_2SO_4 solution at a potential scan rate of 5 mV s^{-1} and an electrode rotating rate of 900 rpm and (b) the calculated data of hydrogen peroxide yield %H_2O_2 and the electron-transfer number *n* in per oxygen molecule.

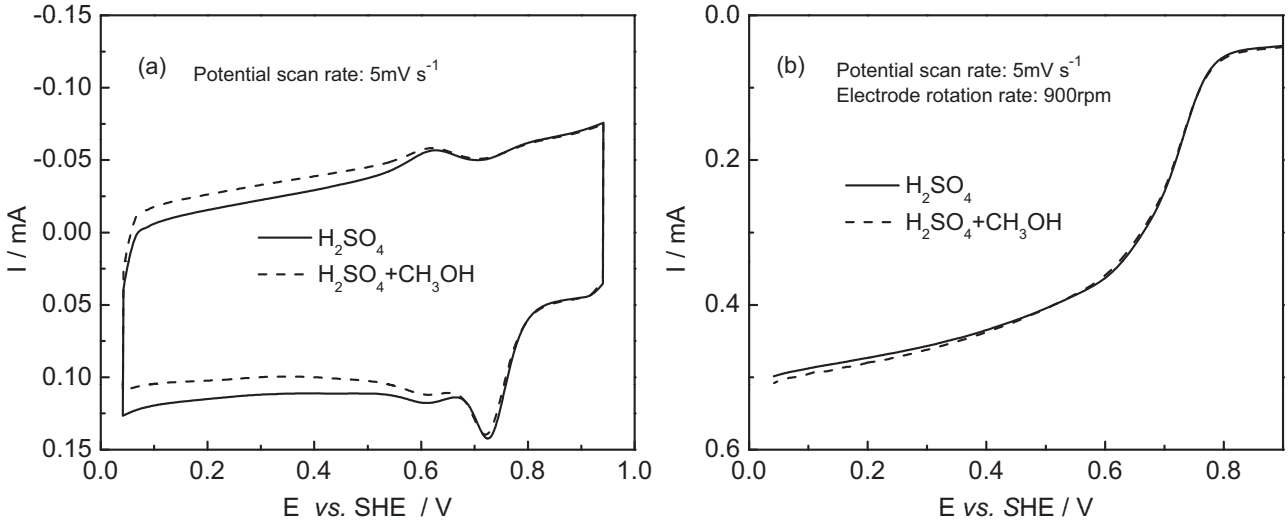

Fig. 9. (a) Cyclic voltammograms and (b) RDE polarization curves of the ORR on HT800 in oxygen-saturated 0.5 M H_2SO_4 solution and 0.5 M H_2SO_4 + 1 M CH_3OH solution.

is more electrocatalytically active than the FeN_4/C [13]. Faubert et al.'s investigations on phthalocyanine and tetraphenylporphyrin derived Fe-N/C catalysts exhibited that the catalytic activity in the catalysts pyrolyzed in the temperature range of 500–700 °C originates from the well dispersed Fe-N_4 moiety or from fragments of the original molecule still containing the metal bound to nitrogen, while there is no Fe—N bond anymore in the catalysts heat-treated at higher temperatures and the metallic Fe surrounded in graphitic envelope works as the active sites [31,32]. Faubert et al.'s study on acetonitrile-based Fe-N/C catalysts showed that either Fe is present in the active site in a high oxidation state unleachable under the form of $FeCl_3$, or that Fe is not a constituent of the active site and its role would be limited to catalyzing the formation of the carbon and nitrogen based active site [23]. Similarly, Oh et al.'s research on polypyrrole/ethylenediamine-based Fe-N/C catalysts indicated that the transition metal itself does not behave as an active site for ORR, but it serves to catalyze the formation of active nitrogen functional groups for the ORR by doping nitrogen into carbon [33]. Kobayashi et al. reported that light elements such as C and N are components of the ORR active sites in the phthalocyanine-based Fe-N/C catalysts pyrolyzed at high temperatures where the metal-N_4 structures in the macrocycles are mostly decomposed, and the residual Fe itself does not seem to contribute directly to the ORR activity [34]. The great discrepancy in the reported active sites is probably, at least in part, resulted from the different preparation of the catalysts, different metal precursors and the different carbon and nitrogen sources used. As for the active site in the FeTETA/C catalysts studied in the present work, we cannot well understand it now. However, according to the results as discussed above that the catalytic activity of FeTETA/C increases with the growing amount of nanometallic Fe in it, we believe that the metallic Fe is involved in the active site in this kind of catalyst.

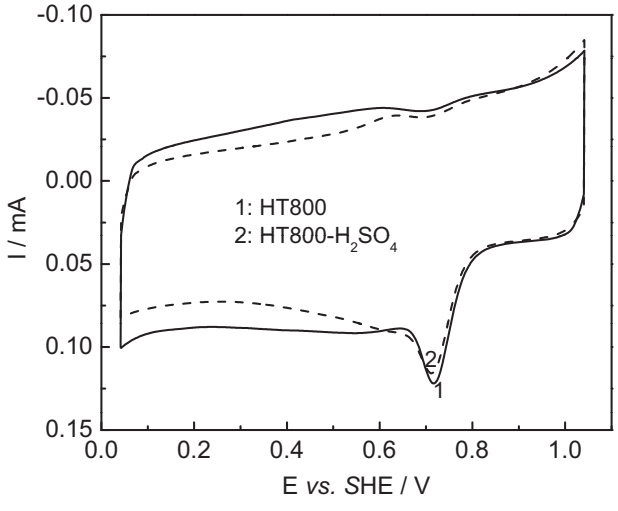

Fig. 10. Cyclic voltammograms of the HT800 catalyst and the HT800-H_2SO_4 catalyst in oxygen-saturated 0.5 M H_2SO_4 solution.

4. Conclusions

A class of non-noble metal catalysts, FeTETA/C, for oxygen reduction have been prepared from pyrolyzing carbon-supported iron triethylenetetramine chelate in Ar atmosphere at diverse temperatures. A powerful influence of heat treatment temperature on catalytic activity of the FeTETA/C catalysts toward ORR have been observed, the ORR catalytic performance increases with increase in heat treatment temperature and reaches the maximum at 800 °C, then it deteriorates with further increase in the temperature. The ORR catalyzed by the optimal catalyst HT800 proceeds through both four-electron-transfer reduction and two-electron-transfer reduction but the former predominates. The optimal catalyst HT800 has excellent methanol-tolerance and acceptable stability. Iron exists mainly as nanoparticulate Fe with excellent crystallization on surface of the FeTETA/C catalysts synthesized in the temperature range from 800 °C to 1000 °C, while lower heat treatment temperature leads to poor Fe crystallization. Both pyridinic N and pyrrolic N could be found in the optimal catalyst, HT800, with more pyridinic type, and oxygen in HT800 is involved in C═O, C—OH and/or C—O—C structures with much more content of C═O.

Acknowledgments

The authors are grateful for the financial support of this work by the National Natural Science Foundation of China (50901086, 51072118, 21176155), Shanghai Rising Star Program (10QA1405000), Shanghai Shuguang Project (09SG46), the STCSM of China (10JC1406900) and Shanghai College Teacher Training Scheme (slg11028).

References

[1] M. Lefèvre, E. Proietti, F. Jaouen, J.P. Dodelet, Iron-based catalysts with improved oxygen reduction activity in polymer electrolyte fuel cells, Science 324 (2009) 71.

[2] H. Jahnke, M. Schönborn, G. Zimmermann, Organic dyestuffs as catalysts for fuel cells, Topics in Current Chemistry 61 (1976) 133.

[3] C.W.B. Bezerra, L. Zhang, K. Lee, H. Liu, A.L.B. Marques, E.P. Marques, H.J. Wang, J. Zhang, A review of Fe-N/C and Co-N/C catalysts for the oxygen reduction reaction, Electrochimica Acta 53 (2008) 4937.

[4] X.Y. Xie, Z.F. Ma, X. Wu, Q. Ren, X. Yuan, Q.Z. Jiang, L.Q. Hu, Preparation and electrochemical characteristics of CoTMPP-TiO_2NT/BP composite electrocatalyst for oxygen reduction reaction, Electrochimica Acta 52 (2007) 2091.

[5] Z.W. Xu, H.J. Li, G.X. Cao, Q.L. Zhang, K.Z. Li, X.N. Zhao, Electrochemical performance of carbon nanotube-supported cobalt phthalocyanine and its nitrogen-rich derivatives for oxygen reduction, Journal of Molecular Catalysis A: Chemical 335 (2011) 89.

[6] S. Pylypenko, S. Mukherjee, T.S. Olson, P. Atanassov, Non-platinum oxygen reduction electrocatalysts based on pyrolyzed transition metal macrocycles, Electrochimica Acta 53 (2008) 7875.

[7] C.W.B. Bezerra, L. Zhang, K. Lee, H. Liu, J. Zhang, Z. Shi, A.L.B. Marques, E.P. Marques, S. Wu, J. Zhang, Novel carbon-supported Fe-N electrocatalysts synthesized through heat treatment of iron tripyridyl triazine complexes for the PEM fuel cell oxygen reduction reaction, Electrochimica Acta 53 (2008) 7703.

[8] T. Okada, M. Yoshida, T. Hirose, K. Kasuga, T. Yu, M. Yuasa, I. Sekine, Oxygen reduction characteristics of graphite electrodes modified with cobalt di-quinolyldiamine derivatives, Electrochimica Acta 45 (2000) 4419.

[9] S.Y. Ye, A.K. Vijh, Non-noble metal-carbonized aerogel composites as electrocatalysts for the oxygen reduction reaction, Electrochemistry Communications 5 (2003) 272.

[10] M. Yuasa, A. Yamaguchi, H. Itsuki, K. Tanaka, M. Yamamoto, K. Oyaizu, Modifying carbon particles with polypyrrole for adsorption of cobalt ions as electrocatatytic site for oxygen reduction, Chemistry of Materials 17 (2005) 4278.

[11] X. Yuan, X. Zeng, H.J. Zhang, Z.F. Ma, C.Y. Wang, Improved performance of proton exchange membrane fuel cells with *p*-toluenesulfonic acid-doped Co-PPy/C as cathode electrocatalyst, Journal of the American Chemical Society 132 (2010) 1754.

[12] H. Liu, Z. Shi, J. Zhang, L. Zhang, J. Zhang, Ultrasonic spray pyrolyzed iron-polypyrrole mesoporous spheres for fuel cell oxygen reduction electrocatalysts, Journal of Materials Chemistry 19 (2009) 468.

[13] M. Lefèvre, J.P. Dodelet, P. Bertrand, Molecular oxygen reduction in PEM fuel cells: evidence for the simultaneous presence of two active sites in Fe-based catalysts, Journal of Physical Chemistry B 106 (2002) 8705.

[14] M. Lefèvre, J.P. Dodelet, P. Bertrand, Molecular oxygen reduction in PEM fuel cell conditions: ToF-SIMS analysis of Co-based electrocatalysts, Journal of Physical Chemistry B 109 (2005) 16718.

[15] H.J. Zhang, X. Yuan, W. Wen, D.Y. Zhang, L.L. Sun, Q.Z. Jiang, Z.F. Ma, Electrochemical performance of a novel CoTETA/C catalyst for the oxygen reduction reaction, Electrochemistry Communications 11 (2009) 206.

[16] H.J. Zhang, X. Yuan, L.L. Sun, X. Zeng, Q.Z. Jiang, Z.P. Shao, Z.F. Ma, Pyrolyzed CoN_4-chelate as electrocatalyst for oxygen reduction reaction in acid media, International Journal of Hydrogen Energy 35 (2010) 2900.

[17] H.J. Zhang, Q.Z. Jiang, L.L. Sun, X. Yuan, Z.P. Shao, Z.F. Ma, 3d non-precious metal-based electrocatalysts for the oxygen reduction reacton, International Journal of Hydrogen Energy 35 (2010) 8295.

[18] H.J. Zhang, X. Yuan, L. Sun, J. Yang, Z.F. Ma, Z. Shao, Synthesis and characterization of non-precious metal binary catalyst for oxygen reduction reaction in proton exchange membrane fuel cells, Electrochimica Acta 77 (2012) 324.

[19] H.J. Zhang, Q.Z. Jiang, L.L. Sun, X. Yuan, Z.P. Shao, Z.F. Ma, Influence of heat treatment on the activity and structure of CoTETA/C catalysts for oxygen reduction reaction, Electrochimica Acta 55 (2010) 1107.

[20] S.Lj. Gojković, S. Gupta, R.F. Savinell, Heat-treated iron(III) tetramethoxyphenyl porphyrin chloride supported on high-area carbon as an electrocatalyst for oxygen reduction: Part III. detection of hydrogen-peroxide during oxygen reduction, Electrochimica Acta 45 (1999) 889.

[21] S.Lj. Gojković, S. Gupta, R.F. Savinell, Heat-treated iron(III) tetramethoxyphenyl porphyrin chloride supported on high-area carbon as an electrocatalyst for oxygen reduction Part II. kinetics of oxygen reduction, Journal of Electroanalytical Chemistry 462 (1999) 63.

[22] P. Gouérec, M. Savy, J. Riga, Oxygen reduction in acid media catalyzed by pyrolyzed cobalt macrocycles dispersed on an active carbon: the importance of the content of oxygen surface groups on the evolution of the chelate structure during the heat treatment, Electrochimica Acta 43 (1998) 743.

[23] G. Faubert, R. Côté, D. Guay, J.P. Dodelet, G. Dénès, C. Poleunis, P. Bertrand, Activation and characterization of Fe-based catalysts for the reduction of oxygen in polymer electrolyte fuel cells, Electrochimica Acta 43 (1998) 1969.

[24] J. Casanovas, J.M. Ricart, J. Rubio, F. Illas, J.M. Jiménez-Mateos, Origin of the Large N 1s Binding Energy in X-ray Photoelectron Spectra of Calcined Carbonaceous Materials, Journal of the American Chemical Society 118 (1996) 8071.

[25] F. Jaouen, S. Marcotte, J.P. Dodelet, G. Lindbergh, Oxygen reduction catalysts for polymer electrolyte fuel cells from the pyrolysis of iron acetate adsorbed on various carbon supports, Journal of Physical Chemistry B 107 (2003) 1376.

[26] N.P. Subramanian, S.P. Kumaraguru, H. Colon-Mercado, H. Kim, B.N. Popov, T. Black, D.A. Chen, Studies on Co-based catalysts supported on modified carbon substrates for PEMFC cathodes, Journal of Power Sources 157 (2006) 56.

[27] R.A. Sidik, A.B. Anderson, N.P. Subramanian, S.P. Kumaraguru, B.N. Popov, O_2 reduction on graphite and nitrogen-doped graphite: experiment and theory, Journal of Physical Chemistry B 110 (2006) 1787.

[28] X. Deng, D. Zhang, X. Wang, X. Yuan, Z.F. Ma, Preparation and catalytic activity of carbon nanotube-supported metallporphyrin electrocatalyst, Chinese Journal of Catalysis 29 (2008) 519.

[29] H.T. Chung, C.M. Johnston, K. Artyushkova, M. Ferrandon, D.J. Myers, P. Zelenay, Cyanamide-derived non-precious metal catalyst for oxygen reduction, Electrochemistry Communications 12 (2010) 1792.

[30] C. Médard, M. Lefèvre, J.P. Dodelet, F. Jaouen, G. Lindbergh, Oxygen reduction by Fe-based catalysts in PEM fuel cell conditions: activity and selectivity of the catalysts obtained with two Fe precursors and various carbon supports, Electrochimica Acta 51 (2006) 3202.

[31] G. Faubert, G. Lalande, R. Côté, D. Guay, J.P. Dodelet, L.T. Weng, P. Bertrand, G. Dénès, Heat-treated iron and cobalt tetraphenylporphyrins adsorbed on carbon black: physical characterization and catalytic properties of these materials for the reduction of oxygen in polymer electrolyte fuel cells, Electrochimica Acta 41 (1996) 1689.

[32] G. Faubert, G. Lalande, R. Côté, D. Guay, J.P. Dodelet, L.T. Weng, P. Bertrand, G. Dénès, Catalytic activity and stability of heat-treated iron phthalocyanines for the electroreduction of oxygen in polymer electrolyte fuel cells, Journal of Power Sources 61 (1996) 227.

[33] H. Oh, H. Kim, The role of transition metals in non-precious nitrogen-modified carbon-based electrocatalysts for oxygen reduction reaction, Journal of Power Sources 212 (2012) 220.

[34] M. Kobayashi, H. Niwa, M. Saito, Y. Harada, M. Oshima, H. Ofuchi, K. Terakura, T. Ikeda, Y. Koshigoe, J. Ozaki, S. Miyata, Indirect contribution of transition metal towards oxygen reduction reaction activity in iron phthalocyanine-based carbon catalysts for polymer electrolyte fuel cells, Electrochimica Acta 74 (2012) 254.